Respiration Monitoring using Doppler-Modulated Depolarizing Chipless Tags

Ashkan Azarfar, Nicolas Barbot, Etienne Perret

Respiration Monitoring using Doppler-Modulated Depolarizing Chipless Tags

Ashkan Azarfar
LCIS, Grenoble INP
University of Grenoble Alpes
Valence, France
ashkan.azarfar@lcis.grenoble-inp.fr

Nicolas Barbot
LCIS, Grenoble INP
University of Grenoble Alpes
Valence, France
nicolas.barbot@lcis.grenoble-inp.fr

Etienne Perret
LCIS, Grenoble INP
University of Grenoble Alpes
Valence, France
etienne.perret@lcis.grenoble-inp.fr

***Abstract*—This paper demonstrates that chipless RFID tags in the depolarizing configuration can be utilized to effectively monitor the human respiration rate and to identify the human subject. The cross-polarized backscattered field from the tag can be isolated from the co-polarized contribution of the human body and the background environment which facilitate the detection and identification process. The measurement principle is also based on the micro-Doppler effect: due to breathing, the movement of the chipless tag modulates the backscattered signal and this modulation is recovered at the reader over large distances. The idea is proved experimentally with measurements done on a human subject in a real environment. The respiration monitoring and the subject identification are achieved at up to 1.8 m read range.**

***Index Terms*—Chipless Radio Frequency IDentification (RFID), Doppler effect, Respiration monitoring**

I. Introduction

Doppler radars have been widely employed in human healthcare monitoring for noncontact detection of respiration and heartbeat rates [1]. In principle, Doppler radars extract the micro-Doppler [2] induced by slight and slow vibration of the human chest or heart, using coherent phase interferometry [3] to estimate the corresponding vibration rate. In recently presented biomedical Doppler radars, carrier frequencies ranging from low microwaves [4] to millimeter waves [5], and different signal processing techniques [6] have been applied to achieve better monitoring performance in terms of accuracy, robustness, and detection range. However, in most cases, the proposed approach suffers from limitations caused by the environment clutter and the presence of other interfering moving objects. To alleviate these limitations and to differentiate the target human body from the other objects, RF tags can be attached to the body to provide specific scattering characteristics which are more detectable than the human body itself. For example, harmonic tags in [7] have been used to detect the micro-Doppler generated around the second harmonic of the carrier frequency while the total contribution of the stationary environment (clutter) and untagged moving objects is rejected in reception by the harmonic radar. Although a robust detection process for respiration monitoring has been achieved in [7] by using the harmonic tag, the large harmonic conversion loss of the tag has caused to limit the read range less than 1 meter, and in addition, the harmonic tag cannot provide the identification capability. On the other hand, it is shown in [8] that moving chipless RFID tags are detectable at larger distances compared to when they are stationary and the read range is limited by the residual environment response [9]. Accordingly, chipless tags attached to the human body may propose an effective way to monitor the respiration rate at larger distances and to identify the target person.

In this paper, we demonstrate that chipless RFID tags composed of depolarizing resonating scatterers can be effectively used for respiration monitoring while the depolarizing property is exploited to isolate the contribution of the tag from that of the environment and other moving objects. In other words, since the human body and most of the objects in the environment have a small cross-polarized scattering parameter [10], the scattering from depolarizing chipless tag can be easily detected using cross-polarized transmitting and receiving antennas. Furthermore, the resonant RCS of the scatterers will improve the read range, and of course, is utilized for the identification goal. Last but not least, the measurement based on the micro-Doppler effect allows to obtain reading distances much higher than those classically reported in the literature for chipless tags.

II. Model and principle description

Fig. 1(a) shows a rectangular loop with the length of L and the width of w in a depolarizing scattering configuration. The loop is assumed in xy-plane while it is rotated around the y-axis by $45°$. The loop is normally impinged by a y-polarized plane wave at the frequency of f_0 expressed as

$$\vec{E}_i = E_y^i \, e^{jkz} \hat{y} \tag{1}$$

where $k = 2\pi f_0/c_0 = 2\pi/\lambda$ and c_0 is the free space light velocity. The scattered field in the normal backscattered direction will have both co-polarized (y) and cross-polarized (x) components which can be written in terms of the incident wave using the polarimetric scattering matrix as

$$\begin{bmatrix} E_x^s \\ E_y^s \end{bmatrix} = \begin{bmatrix} S_{xx} & S_{xy} \\ S_{yx} & S_{yy} \end{bmatrix} \begin{bmatrix} E_x^i \\ E_y^i \end{bmatrix} \tag{2}$$

For $w \ll L$, the fundamental resonance of the loop occurs when $L = \lambda/2$. Since in this configuration both the folded dipole mode and the transmission line mode of the rectangular

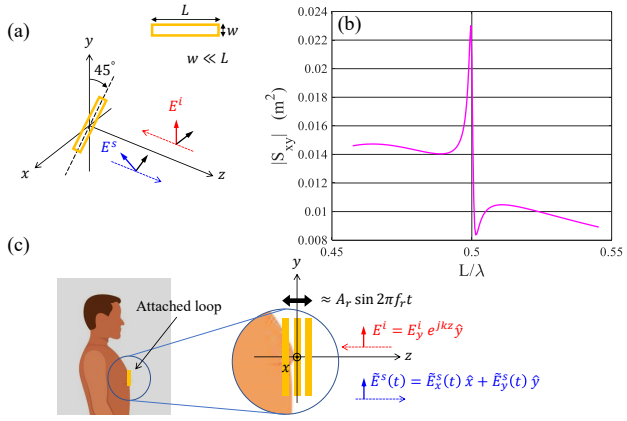

Fig. 1. (a) Rectangular loop in the depolarizing scattering configuration. (b) The cross-polarized scattering parameter of the depolarizing loop around the fundamental resonant mode. (c) Scattering from depolarizing loop attached to the human chest.

loop [11] is excited, the cross-polarized scattering parameter of the loop S_{xy} have a sharp resonance associated to the transmission line mode as it is shown in Fig. 1(b) while the less resonant contribution of the folded dipole model can be also observed beyond the sharp resonance ($L/\lambda = 0.5$). However, in this work, only the sharp resonance of S_{xy} is considered for development. Suppose that the rectangular loop is attached to the human chest in the depolarizing configuration as it is illustrated in Fig. 1(c). The slight movement of the chest due to the respiration can be considered as a sinusoidal vibration $A_r \sin 2\pi f_r t$ where A_r and f_r are respectively associated to the depth and rate of the respiration. Using the classical micro-Doppler formulation presented in [2], the cross-polarized component of the phase-modulated backscattered field is almost generated only by the loop, which can be derived as

$$\tilde{E}^s_x(t) = \frac{S_{xy}(f_0) E^i_y\, e^{-jkz}}{z}\, e^{j2kA_r \sin 2\pi f_r t)} \tag{3}$$

In addition, the total co-polarized scattered field generated by the loop, human body, and the background environment can be modeled as $\tilde{E}^s_y(t)$ [Fig. 1(c)]. Accordingly, by using two linearly polarized antennas as the transmitter and receiver in the cross configuration, it is possible to capture only the cross-polarized component $\tilde{E}^s_x(t)$ while the received signal is not affected by the co-polarized scattered field. This is the key point which can be used to provide isolation between the contribution of the depolarizing tag and that of all the other objects, and to reach better respiration monitoring performance compared to what has been done without using a tag. The frequency representation of (3) can be obtained as

$$\tilde{\mathbf{E}}^s_x(f) = \frac{S_{xy}(f_0) E^i_y\, e^{-jkz}}{z} \sum_{n=-\infty}^{+\infty} J_n(\beta)\delta(f - nf_r) \tag{4}$$

where $\beta = 4\pi A_r/\lambda$ and J_n is the first kind Bessel function of order n.

The differential Radar Cross Section (RCS) σ_d of the moving chipless tags has been introduced in [8]. Accordingly, the σ_d associated to the cross-component of the backscattered field ($\tilde{E}^s_x$) can be written as

$$\sigma_d(f_0) = 4\pi |S_{xy}(f_0)|^2 (1 - [J_0(\beta)]^2) \tag{5}$$

which is directly proportional to $|S_{xy}|^2$, and make it possible to identify the resonance frequency of the attached loop in terms of calculated differential RCS by measuring the backscattered signal in different carrier frequencies.

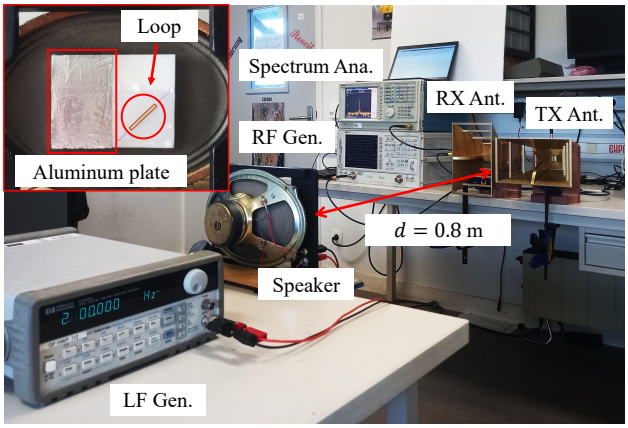

Fig. 2. Measurement bench used for verifying the idea based on the vibration generated by the loudspeaker.

III. Results

A. Experimental verification using loudspeaker

The measurement bench used to verify the proposed idea is presented in Fig. 2 where all the measurements have been done in a real environment in the laboratory. The setup is composed of two linearly polarized transmitting and receiving antennas (A.H. Systems SAS-571) which are configured in cross, and they are respectively connected to the RF signal generator (HP 8720D in CW mode) and the spectrum analyzer (Tektronix RSA3408A). The RF generator and the spectrum have been synchronized using a common 10 MHz reference signal to realize a coherent reception which is essential to preserve the small phase modulation induced by the respiration. A sequence of CW signals ranging from $4.6 - 5$ GHz with the power of $P_t = 0$ dBm is injected to the transmitting antenna, and the received signal is acquired by the spectrum analyzer through the span of 30 Hz. A loudspeaker is positioned in front of the antennas at $d = 0.8$ m distance while it is excited with a LF signal generator at $f_r = 2$ Hz to realize a respiration model. The approximate amplitude of the vibration produced by the speaker at this frequency is less than 1 mm. The speaker is attached with a foam support which is half covered by a piece of aluminum tape and the loop is positioned on it in a depolarizing configuration as it is shown in the inset of Fig. 2. The loop is made of 100 μm copper wire with $L = 28.4$ mm and $w = 3$ mm, and its resonance frequency is measured as 4.81 GHz.

The cross-component of the backscattered field is measured at the resonance frequency of the loop for three cases in

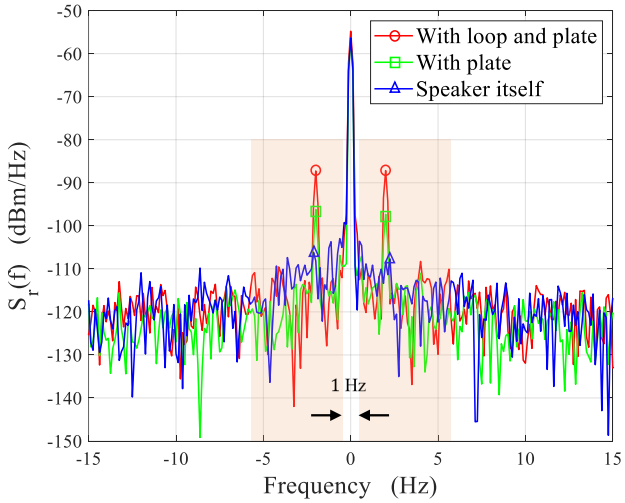

Fig. 3. The measured PSD of the signal backscattered from the speaker with the attached depolarizing loop and aluminum plate.

which the target are (I) speaker itself with the foam support, (II) speaker when the aluminum plate is attached to the foam support, and (III) speaker with the plate and loop both attached. The measured Power Spectral Density (PSD) of the received signal $S_r(f)$ for theses three cases are shown in Fig. 3. As it can be observed clearly, the levels of the micro-Doppler harmonics for when the loop is attached are at least 10 dB greater than when it is not attached. Therefore, this experiment proves that the depolarizing loop can be detected effectively at large distances for respiration monitoring goal.

To demonstrate the identification capability, the measurement have been done for $f_0 = [4600 : 10 : 5000]$ MHz, and the modulated backscattered power $P_{bs\,d}$ is calculated by integrating $S_r(f)$ over the bandwidth highlighted in Fig. 3 at each carrier frequency, and the associated differential RCS is obtained by

$$\sigma_d(f_0) = \frac{(4\pi)^3 d^4 P_{bs\,d}}{\lambda^2 G_r G_t P_t} \tag{6}$$

where G_t and G_r are respectively the transmitting and receiving antenna gain. The calculated differential RCS (σ_d) as a function of carrier frequency (f_0) for the three cases (I),(II), and (III) are presented in Fig. 4(a). Obviously, the value of differential RCS for when the loop is attached is higher, and the sharp resonance of the loop can be detected based on the measured σ_d as it has been predicted by (5). To show more clearly the validity of (5), the measured differential RCS is compared with the result obtained from simulation in terms of the cross-polarized scattering parameter (S_{xy}) in Fig. 4(b). The measured data is in accord with the simulation results in terms of behaviour, and using (5) the corresponding β value and the amplitude of vibration can be respectively estimated as 0.02 and 0.21 mm which are in agreement with what has been mentioned previously.

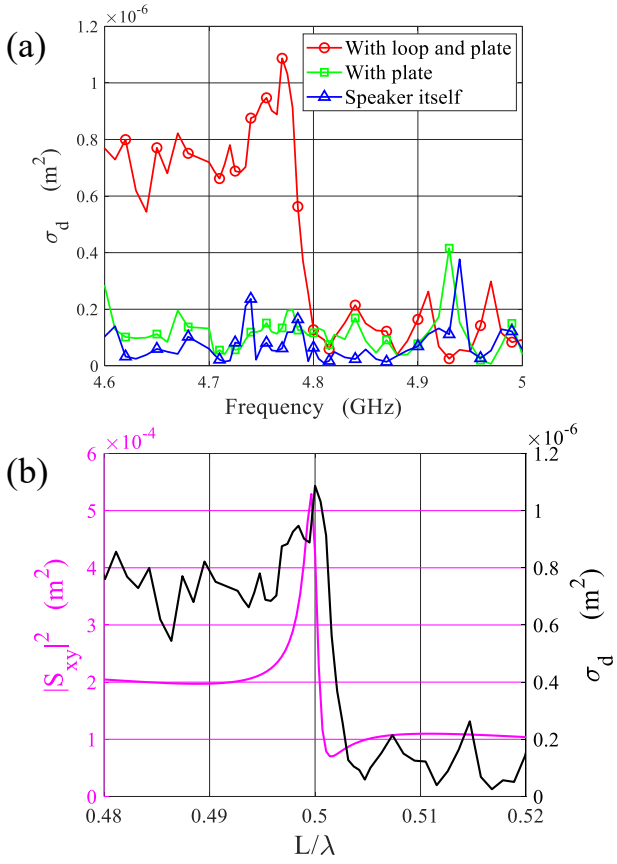

Fig. 4. (a) Calculated differential RCS based on the measured PSD as a function of carrier frequency for the speaker with the attached depolarizing loop and aluminum plate. (b) Measured differential RCS of the vibrating depolarizing loop in comparison with the magnitude square of the cross-polarized scattering parameter obtained in simulation [See Equation (5)].

B. Respiration monitoring with identification capability

The performance of the respiration monitoring using the depolarizing chipless tag (rectangular loop) has been tested on a human subject in the real environment as it is presented by Fig. 5. Using the same setup as described previously, the measurements have been done while the human subject was sitting at $d = 1.8$ m and the depolarizing loop was attached to his chest using a belt as it is shown in the inset of Fig. 5. Due to the performance limitations of the used equipment (RF generator and spectrum analyzer) in terms of phase noise and minimum acquisition span, the human subject was breathing a little faster and deeper than the natural respiration manner during the measurement.

At the resonance frequency of the loop, the captured signals are illustrated in Fig. 6(a) for three cases namely human subject himself, human subject wearing the belt, and human subject wearing the belt with attached depolarizing loop. Considering the observed micro-Doppler harmonics of the respiration rate and their corresponding levels in each case, the detection process and the respiration rate monitoring performance are significantly improved in terms of accuracy and achievable read range by using the depolarizing chipless tag.

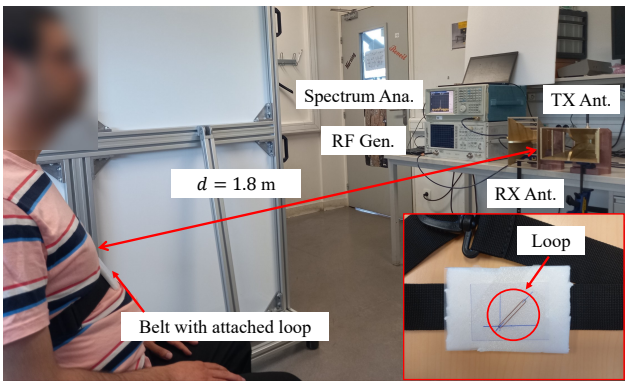

Fig. 5. Respiration monitoring and human subject identification in the real environment using depolarizing loop attached to the body.

The measured respiration rate of the human subject is 1.2 Hz. Moreover, the resonance frequency of the loop is identified during the respiration based on the calculated differential RCS. The calculated σ_d for the three cases as a function of carrier frequency are depicted in Fig. 6(b) while the resonance of the loop can be detected for when the tag is attached to the body, and accordingly it is possible to identify the target human subject when he or she wears the tag. It should be mentioned that the observed fluctuations for the calculated differential RCS in Fig. 6(b) can be suppressed if the measurement is done at the same time for all the carrier frequencies. In this way, the results will not be affected by the variation of the body movements and breathing situation of the human subject during several minutes of measurement.

IV. Conclusion

The respiration monitoring using depolarizing chipless tag based on micro-Doppler measurement has been demonstrated and verified experimentally. A model has been proposed to describe the benefit of using depolarizing chipless tags in terms of robust detection, and the identification process has been established based on it. For a human subject in a real environment, the respiration rate has been accurately measured at 1.8 m distance while the target person is also identified.

Acknowledgment

This work was supported by the European Research Council (ERC) through the European Union's Horizon 2020 Research and Innovation Program (ScattererID) under Grant N° 772539.

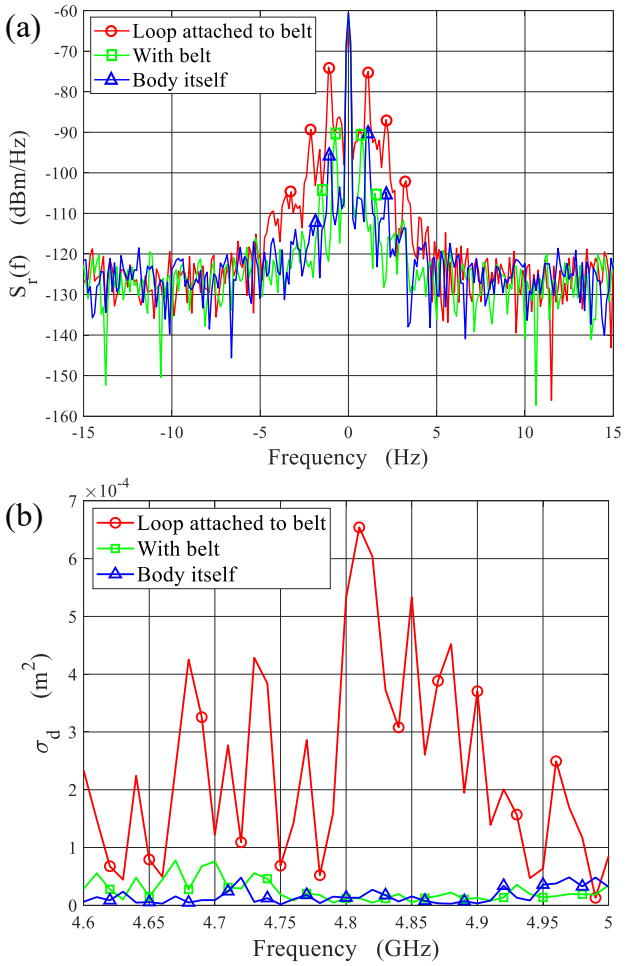

Fig. 6. (a) The measured PSD of the signal backscattered from human subject during respiration with and without attached depolarizing loop on the chest. (b) Calculated differential RCS based on the measured PSD as a function of carrier frequency for human subject during respiration with and without attached depolarizing loop on the chest.

References

[1] C. Li, V. M. Lubecke, O. Boric-Lubecke, and J. Lin, "A review on recent advances in Doppler radar sensors for noncontact healthcare monitoring," *IEEE Trans. Microw. Theory Techn.*, vol. 61, no. 5, pp. 2046–2060, 2013.

[2] V. C. Chen, F. Li, S. . Ho, and H. Wechsler, "Micro-Doppler effect in radar: phenomenon, model, and simulation study," *IEEE Trans. Aerosp. Electron. Syst.*, vol. 42, no. 1, pp. 2–21, Jan. 2006.

[3] S. Kim and C. Nguyen, "A displacement measurement technique using millimeter-wave interferometry," *IEEE Transactions on Microwave Theory and Techniques*, vol. 51, no. 6, pp. 1724–1728, 2003.

[4] K.-M. Chen, Y. Huang, J. Zhang, and A. Norman, "Microwave life-detection systems for searching human subjects under earthquake rubble or behind barrier," *IEEE transactions on biomedical engineering*, vol. 47, no. 1, pp. 105–114, 2000.

[5] D. T. Petkie, C. Benton, and E. Bryan, "Millimeter wave radar for remote measurement of vital signs," in *2009 IEEE Radar Conference*. IEEE, 2009, pp. 1–3.

[6] C. Li and J. Lin, "Random body movement cancellation in Doppler radar vital sign detection," *IEEE Transactions on Microwave Theory and Techniques*, vol. 56, no. 12, pp. 3143–3152, 2008.

[7] A. Singh and V. M. Lubecke, "Respiratory monitoring and clutter rejection using a CW Doppler radar with passive RF tags," *IEEE Sensors Journal*, vol. 12, no. 3, pp. 558–565, 2011.

[8] A. Azarfar, N. Barbot, and E. Perret, "Chipless RFID based on micro-Doppler effect," *IEEE Transactions on Microwave Theory and Techniques*, vol. 70, no. 1, pp. 766–778, 2021.

[9] N. Barbot, O. Rance, and E. Perret, "Classical RFID versus chipless RFID read range: Is linearity a friend or a foe?" *IEEE Transactions on Microwave Theory and Techniques*, vol. 69, no. 9, pp. 4199–4208, 2021.

[10] A. Vena, E. Perret, and S. Tedjni, "A depolarizing chipless RFID tag for robust detection and its FCC compliant UWB reading system," *IEEE transactions on microwave theory and techniques*, vol. 61, no. 8, pp. 2982–2994, 2013.

[11] R. King, "The rectangular loop antenna as a dipole," *IRE Transactions on Antennas and Propagation*, vol. 7, no. 1, pp. 53–61, 1959.